

Control of morphogenesis and actin localization by the *Penicillium marneffe* RAC homolog

Kylie J. Boyce, Michael J. Hynes and Alex Andrianopoulos*

Department of Genetics, University of Melbourne, Victoria 3010, Australia

*Author for correspondence (e-mail: alex.a@unimelb.edu.au)

Accepted 11 December 2002

Journal of Cell Science 116, 1249-1260 © 2003 The Company of Biologists Ltd
doi:10.1242/jcs.00319

Summary

Rac proteins control polarized growth in many organisms but the specific function of these proteins remains undefined. In this study, we describe the cloning and functional characterization of a RAC homolog, *cf1B*, from the dimorphic fungus *Penicillium marneffe*. *P. marneffe* produces asexual spores on complex structures (conidiophores) and switches between hyphal and yeast growth. *Cf1B* colocalizes with actin at the tips of vegetative hyphal cells and at sites of cell division. Deletion of *cf1B* results in cell division (septation) and growth defects in both vegetative hyphal and conidiophore cell types such that cells become depolarized, exhibit inappropriate septation and the actin cytoskeleton is severely disrupted. This data suggests that Rac proteins play a crucial role in

actin dependent polarized growth and division. The CDC42 ortholog in *P. marneffe*, *cf1A*, controls vegetative hyphal and yeast growth polarization but does not affect asexual development. By contrast, *Cf1B* affects cellular polarization during asexual development and hyphal growth but not during yeast growth. This shows that these two GTPases have both overlapping and distinct roles during growth and development. RAC orthologs are not found in less morphologically complex eukaryotes such as *Saccharomyces cerevisiae*, suggesting that RAC genes might have evolved with increasing cellular complexity.

Key words: RAC, *Penicillium marneffe*, Polarization, Fungal pathogen, Actin

Introduction

The ability of cells to reorganize their cytoskeleton dynamically is crucial for rapid morphological responses to the environment. In addition, the differentiation of morphologically distinct cell types during development requires changes in cytoskeletal organization. Proteins that play an important role in regulating the organization of the actin component of the cytoskeleton include the Ras and Rho GTPases, including Rho, Cdc42 and Rac. These proteins act as molecular switches, responding to upstream signals to localize or activate proteins associated with polarized growth. Small GTPases cycle between an inactive GDP-bound state and an active GTP-bound state. The transition between the GDP- and GTP-bound states is controlled by guanine-nucleotide-exchange factors (GEFs) and GTPase-activating proteins (GAPs) (reviewed in Chant and Stowers, 1995). Mutations have been identified that result in an inability to exchange GDP for GTP, thus rendering the GTPase inactive. Dominance can arise from sequestration of the GEF by the mutant protein, resulting in a dominant negative phenotype. Mutations have also been isolated which produce a constitutively activated protein and a consequent dominant activated phenotype (Davis et al., 1998). These mutations have been used to elucidate the role of small GTPases in many organisms.

Of significant interest is the role of the Rho-family GTPase Rac because, unlike the other Rho GTPases, Rac orthologs are not present in either *Saccharomyces cerevisiae* or *Schizosaccharomyces pombe* and very little is known about the specific role played by this GTPase. In higher eukaryotes, a

general role of Rac proteins is to regulate cellular morphogenesis (Johnson, 1999). Inappropriate function of the RAC homolog in *Drosophila melanogaster* affects morphogenesis by resulting in defects in axon initiation and elongation during nervous-system development, duplication of wing hairs during wing-hair development, loss of photoreceptor differentiation during eye development and randomized ommatidial rotation and misorientation (Eaton et al., 1995; Fanto et al., 2000; Luo et al., 1994).

Defects in morphogenesis in Rac mutants of some organisms have been shown to be a direct consequence of the loss of correct actin organization. Expression of the dominant-negative form of the *Arabidopsis thaliana* Rac homolog in tobacco (*Nicotiana tabacum*) results in a reduction of actin bundles and inhibition of pollen-tube elongation. In the constitutively active form, the mutant protein leads to cellular depolarization with excessive actin cables (Kost et al., 1999). In mammalian cells, the formation of actin-rich cell extensions termed lamellipodia is dependent on induction by Rac. The dominant activated protein induces the formation of lamellipodia, whereas the dominant-negative form blocks lamellipodia formation (Nobes and Hall, 1995).

Fungi represent a highly amenable eukaryotic system in which to study polarized growth and development. *Penicillium marneffe* is an opportunistic human pathogen that is dimorphic, capable of growing in a filamentous multinucleate hyphal form at 25°C or as a uninucleate pathogenic yeast form at 37°C. Upon switching from hyphal growth at 25°C to yeast growth at 37°C, *P. marneffe* undergoes a process termed arthroconidiation. Double septa (cross walls) are laid down

along the arthroconidiating hyphae and fragmentation occurs along the septal plane to generate single cells. Liberated yeast cells are uninucleate and divide by fission (Chan and Chow, 1990). Switching from yeast growth at 37°C to hyphal growth at 25°C requires the polarized growth of yeast cells, septation, branching and the uncoupling of nuclear and cellular division to produce multinucleate cells, which form the multinucleate hyphal mycelium characteristic of *P. marneffei* at 25°C. The two growth forms possess unique modes of polarized growth. In addition to dimorphic growth, *P. marneffei* also undergoes an asexual developmental program at 25°C. This complex developmental process requires the differentiation of multiple specialized cell types that form a structure termed a conidiophore. This differentiation process culminates in the production of uninucleate asexual spores (conidia) from highly specialized sporogenous cells. Asexual development also requires changes in polarized growth that are distinct from those required for hyphal or yeast growth.

Previously, we identified and characterized the *P. marneffei*

CDC42 homolog, *cflA* (*CDC42-like gene A*). Correct CflA function is required for polarized growth of vegetative hyphae at 25°C and yeast cell morphogenesis at 37°C. By contrast, *cflA* was not involved in asexual development at 25°C and no other regulator of polarized growth during asexual development was known (Boyce et al., 2001). During the cloning of *cflA*, a second related gene was identified, designated *cflB*, which has been found to encode another Rho GTPase, with specific homology to the *RAC* class. There has been no functional characterization of a *RAC* homolog in a morphologically complex fungal species to date. The *RAC* homolog *YIRAC1* has been cloned from the dimorphic yeast *Yarrowia lipolytica*, and deletion results in defects in cell morphology and impairment of hyphal growth (Hurtado et al., 2000). In this study, we have investigated the role of the *RAC* homolog *cflB* in the growth and development of *P. marneffei*. CflB is localized to plasma and internal membranes, and to septa in live cells, and co-localizes with actin at nascent septation sites and at the hyphal apex. By generating *cflB* gene deletion and *cflB* dominant-

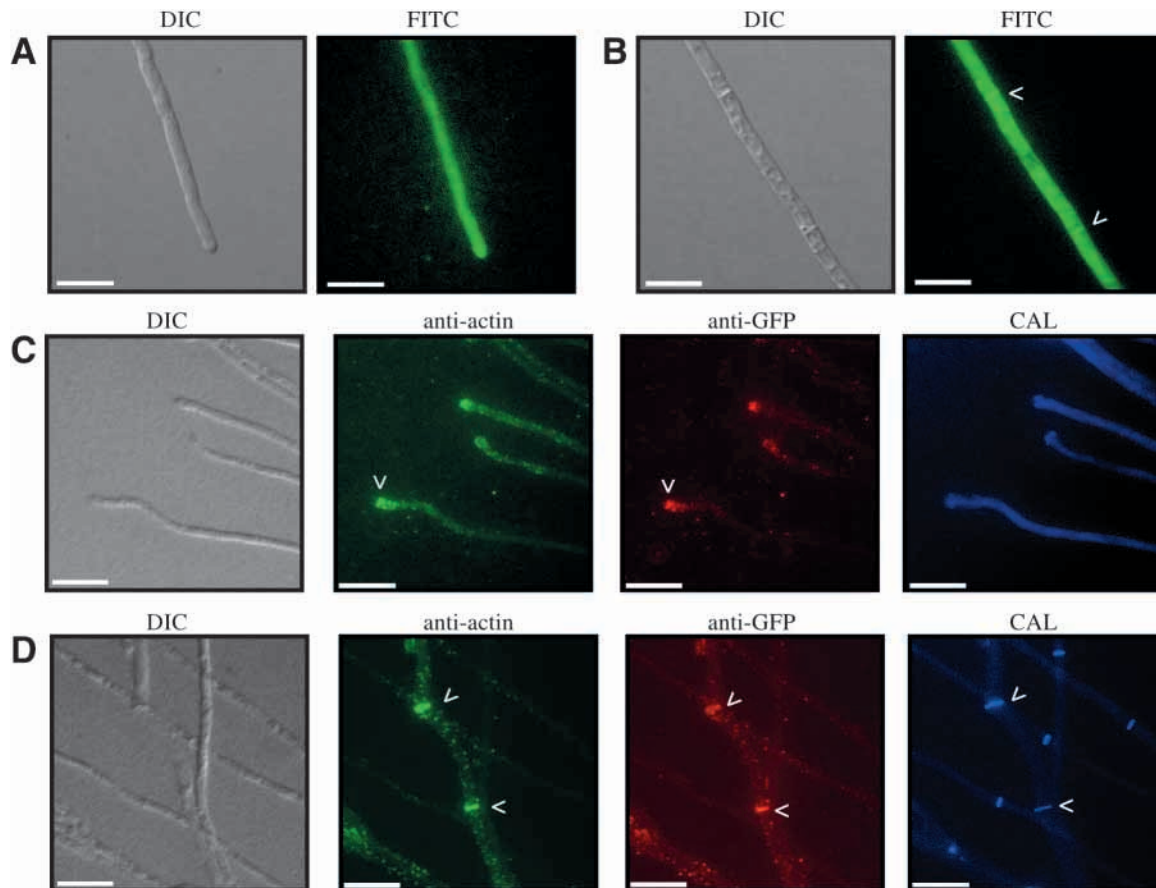


Fig. 1. The *cflB* gene is localized to the plasma and internal membranes, and co-localizes with actin. The *gpdA(pgfp)::cflB* strains were grown for 2 days at 25°C. CflB visualized in live cells (A,B) and in fixed cells by immunocytochemistry (C,D). (A) Apical hyphal cells. The GFP::CflB fusion protein is not present in large amounts at the hyphal apex. (B) Subapical hyphal cells. The GFP::CflB fusion protein is localized at the plasma membrane, at internal membranes and at septation sites. The single white arrows indicate the GFP::CflB fusion protein localized at septa. (C) CflB co-localizes with actin at the hyphal apex. Actin is concentrated at sites of polarized growth, such as the hyphal apex, indicated by the white arrow (anti-actin). The GFP::CflB fusion protein co-localizes with actin at the hyphal apex, shown by the white arrow (anti-GFP). (D) CflB co-localizes with actin at nascent septation sites. Actin is localized at nascent septation sites, indicated by white arrows (anti-actin). The white arrows under anti-GFP and CAL staining indicate the GFP::CflB fusion protein, which also localizes at nascent septation sites, and the corresponding cell walls, respectively. Scale bars, 20 µm.

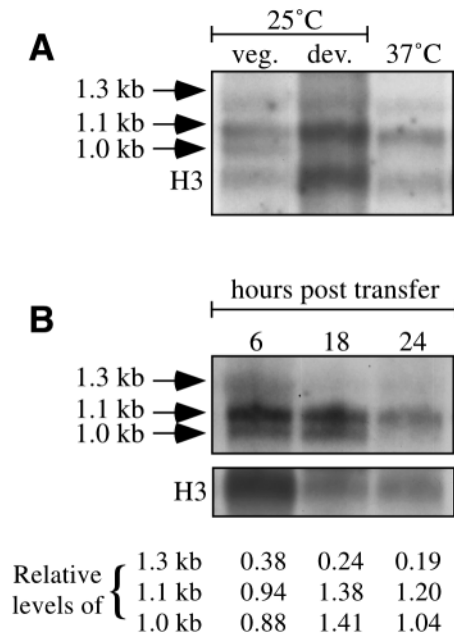


Fig. 2. The *cflB* gene is expressed as three transcripts at both 25°C and 37°C. (A) Northern-blot analysis of *cflB* expression. Total RNA was isolated from vegetatively growing hyphae at 25°C (veg.), asexually developing cultures at 25°C (dev.) and yeast cells (37°C). Northern blots were probed with *cflB* and a histone H3 probe as a RNA loading control. Arrows indicate the three *cflB* transcripts, and the histone H3 is marked. (B) Northern-blot analysis using total RNA isolated during the dimorphic switching from yeast to hyphae. Yeast cells produced at 37°C were transferred to 25°C and total RNA isolated at 6 hours, 18 hours and 24 hours after transfer. Northern blots were probed with *cflB* and a histone H3 probe as an RNA loading control. Arrows indicate the three *cflB* transcripts, and the histone H3 is marked. The relative levels of the three *cflB* transcripts are shown. Transcript levels were determined by densitometry and normalized relative to the H3 loading control.

negative and dominant-activated strains, we have shown that CflB is required for the morphogenesis of conidiophores during asexual development in both *P. marneffei* and *Aspergillus nidulans* and show that the mechanisms regulating polarized growth in these two fungal species differ. CflB also plays an overlapping but distinct role to CflA in polarized growth during vegetative hyphal growth. We also show that CflB is required for correct actin localization in vegetative and asexual cells at 25°C.

Of significant interest, is the discovery that, unlike the *CDC42* homolog *cflA*, *cflB* is required for cellular polarization during asexual development but is not involved in yeast cell production at 37°C. Our results indicate that, although small GTPases play similar roles in morphogenesis and actin organization, each protein has a specialized and distinct role during development.

Materials and Methods

Molecular techniques

Plasmid DNA was isolated using the Roche High Purity Plasmid kit. Genomic DNA from *P. marneffei* and *A. nidulans* was isolated as previously described (Borneman et al., 2001). RNA was prepared

using the FastRNA kit from Bio101 as previously described (Borneman et al., 2000). RNA was isolated from vegetative hyphal cells grown at 25°C for 2 days in liquid medium, from asexually developing cultures grown on solid medium at 25°C for 4 days and from yeast cells grown at 37°C for 8 days in liquid medium. Southern and northern blotting were performed with Amersham Hybond N+ membrane according to the manufacturer's instructions. Filters were hybridized using [α -³²P]dATP-labelled probes using standard methods (Sambrook et al., 1989).

Cloning and plasmid construction

A *P. marneffei* genomic library was constructed by ligating partially *Sau3AI*-digested *P. marneffei* genomic DNA into *Bam*HI-digested λ GEM-11 and screened at low stringency (50% formamide, 2 \times SSC, 37°C) for Rho GTPase homologs using *P. marneffei cflA* (a *CDC42* homolog). A weakly hybridizing clone was isolated and a 3.5 kb *Sac*I/*Eco*RI-hybridizing genomic fragment was cloned into pGEM3ZF to generate pKB4811. Sequencing was performed by the Australian Genome Research Facility and sequence was analysed using SequencherTM 3.1.1 (Gene Codes). The Genbank accession number of the *P. marneffei cflB* gene is AF515698. Database searches and sequence comparison were performed using the Australian National Genomic Information Service. A cDNA library, constructed using the SMART cDNA Library construction kit (Clontech Laboratories) with RNA isolated from a 37°C vegetative culture (Borneman et al., 2000) was probed with a 2.5 kb *Spe*I/*Eco*RI fragment of *cflB* (50% formamide, 0.1 \times SSC, 37°C).

The *cflB* deletion construct (pKB4947) was generated by replacing the *Eco*RV/*Sal*I fragment (+183 bp to +308 bp relative to the start codon) of the *Spe*I/*Eco*RI *cflB* subclone pKB4883 with a 2.3 kb *Sma*I/*Xho*I fragment containing the *A. nidulans pyrG*⁺ selectable marker. The *cflB* gene (−182 to +813) was amplified by PCR using the primers F79 (5'-GAG GTA CCT GAG CAT TTA TAC GGG TG-3') and F80 (5'-GAG GAT CCC ATA TAC GCA GTA GGA TAG-3'), digested with *Kpn*I/*Bam*HI and ligated into the pAL3 vector containing the *A. nidulans alcA* promoter (May, 1987) to yield the *alcA(p)::cflB* overexpression construct (pKB5021). To generate the *alcA(p)::cflB*^{D123A} construct, the D123A mutagenic primer J21 (5'-CAC TAA GCT TGC TTT GAG AG-3') and the M13-20 forward primer were used to amplify from +515 to +1593 of *cflB*, from which a 0.64 kb *Hind*III fragment containing the mutation was used to replace the equivalent fragment in a *alcA(p)::cflB* subclone (pKB5021), generating pKB5266. To generate the *alcA(p)::cflB*^{G18V} construct, the G18V mutagenic primer J20 (5'-GGT GAC CGG TGA TGT TGC TG-3') and the M13-20 forward primer were used to amplify from +98 to +1593 of *cflB*, from which a 0.86 kb *Age*I fragment containing the mutation was used to replace the equivalent fragment in a *alcA(p)::cflB* subclone (pKB5021) generating pKB5263. The integrity of the constructs was confirmed by sequencing. The *cflB* gene, from −1 to +813 was amplified by PCR using the primers J55 (5'-CGA GCT CAA TGG CGT CTG GGC-3') and F80 (5'-GAG GAT CCC ATA TAC GCA GTA GGA TAG-3'), digested with *Eco*CR1/*Bam*HI and the 0.9 kb fragment ligated into the *Sma*I/*Bam*HI-digested pAA4240 vector containing the constitutive *gpd* promoter and *GFP* to yield the *gpdA(p)::gfp::cflB* construct (pKB5441).

Fungal strains and media

P. marneffei strains FRR2161, SPM3 and SPM4, and the DNA-mediated transformation process have been described previously (Borneman et al., 2001). The *gpdA(p)::gfp::cflB* strains were generated by co-transformation of SPM4 with pKB5441 [*gpdA(p)::gfp::cflB*] and the *pyrG* selectable plasmid pAB4342. The *alcA(p)::cflB*, *alcA(p)::cflB*^{G18V} and *alcA(p)::cflB*^{D123A} strains were generated by transformation of SPM4 with pKB5021 [*alcA(p)::cflB*],

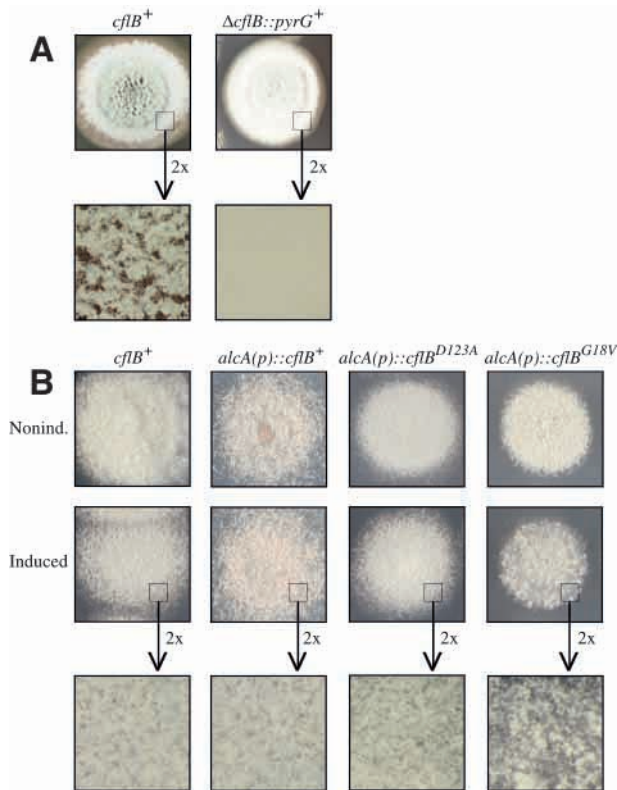


Fig. 3. Colonial morphology of *P. marneffei* *cflB* strains. (A) Colonial morphology of the *P. marneffei* $\Delta cflB$ strain compared with the parental SPM4 control strain ($cflB^+$). Strains were grown at 25°C for 14 days. The $\Delta cflB$ colonies have a fluffy phenotype with reduced conidiation. At higher magnification (2 \times), no conidiophore structures were evident in the $\Delta cflB$ strain. (B) Colonial morphology of *P. marneffei* *cflB* mutant transformants. Strains were grown for 12 days at 25°C on noninducing (Nonind.) or inducing medium (Induced). The $alcA(p)::cflB^{D123A}$ dominant-negative transformants displayed reduced conidiation and an increase in the number of aerial hyphae under inducing conditions and the $alcA(p)::cflB^{G18V}$ dominant-activated transformants displayed patchy conidiation that is more apparent when viewed under higher magnification (2 \times).

pKB5266 [$alcA(p)::cflB^{D123A}$] or pKB5263 [$alcA(p)::cflB^{G18V}$] and selecting directly for $pyrG^+$. The $\Delta cflB::pyrG^+$ strain was generated by transforming SPM4 with linearized pKB4947 and selecting for $pyrG^+$. Transformants were then screened by Southern-blot analysis. The $\Delta cflB::pyrG^-$ strain was isolated by growth of the $\Delta cflB::pyrG^+$ strain on 5-fluororotic acid (5-FOA) medium containing uridine and uracil to select for loss of the $pyrG$ marker. A 5-FOA-resistant sector was isolated and had a restriction map consistent with loss of $pyrG$ at the *cflB* locus. This strain is unable to grow in the absence of uridine (5 mM) and uracil (5 mM).

The *A. nidulans* strains were generated by transformation with pKB5021 [$alcA(p)::cflB$], pKB5266 [$alcA(p)::cflB^{D123A}$] and pKB5263 [$alcA(p)::cflB^{G18V}$] and selecting directly for $pyrG^+$.

At 25°C, strains were grown on ANM (*Aspergillus nidulans* medium) supplemented with 10 mM γ -amino butyric acid (GABA) as a sole nitrogen source (Cove et al., 1966). At 37°C, strains were grown on either brain-heart infusion (BHI) or synthetic dextrose (SD) medium. The $gpdA(p)::gfp::cflB$ strains were grown in liquid SD medium at 37°C (Ausubel et al., 1994). The $alcA(p)::cflB$, $alcA(p)::cflB^{D123A}$ and $alcA(p)::cflB^{G18V}$ strains were grown on carbon-free medium (CF) (Cove et al., 1966) with GABA and fructose

(uninduced conditions) or on CF with GABA, fructose and cyclopentone (induced conditions).

Microscopy

P. marneffei strains were grown on slides covered with a thin layer of solid medium and with one end resting in liquid medium (Borneman et al., 2000).

At 25°C, $alcA(p)::cflB$, $alcA(p)::cflB^{D123A}$ and $alcA(p)::cflB^{G18V}$ strains were grown in liquid CF medium with 0.1% glucose and 10 mM GABA for 1 or 2 days, and induced by replacement of the medium with CF medium containing 0.1 M cyclopentone and 0.1% fructose, and incubating for an additional 1 or 2 days. The $\Delta cflB::pyrG$ strain was grown on ANM supplemented with GABA at 25°C for 2 or 4 days.

At 37°C $alcA(p)::cflB$, $alcA(p)::cflB^{D123A}$ and $alcA(p)::cflB^{G18V}$ strains were grown for 4 days at 37°C on slides coated with BHI and resting in BHI liquid medium before replacement of the medium with 0.1 M cyclopentone and 0.1% fructose for an additional 2 days. The $\Delta cflB::pyrG$ strain was grown on BHI medium for 4 days at 37°C.

Immunofluorescence microscopy for detection of the actin cytoskeleton was performed using standard protocols (Fischer and Timberlake, 1995). Mouse C4 monoclonal anti-actin antibody (Chemicon International) diluted at 1:200 was the primary antibody and ALEXA 488 rabbit anti-mouse antibody (Molecular Probes) at a 1:1000 dilution was the secondary antibody. Immunofluorescence microscopy for detection of the actin cytoskeleton and CflB was performed using standard protocols on two $gpd(p)::gfp::cflB$ strains (Fischer and Timberlake, 1995). Mouse C4 monoclonal anti-actin antibody (1:200 dilution) and rabbit polyclonal anti-green-fluorescent-protein (GFP) antibody (1:50 dilution) were the primary antibodies and ALEXA 488 rabbit anti-mouse antibody (1:1000 dilution) and ALEXA 594 goat anti-rabbit antibody (1:500 dilution, Molecular Probes) were the secondary antibodies. The FRR2161 wild-type strain, the $gpd(p)::gfp::cflB$ strains and the $\Delta cflB$ strain were grown on ANM plus GABA slides for 4 days at 25°C and the FRR2161 and the $\Delta cflB$ strain also grown on SD slides for 4 days at 37°C.

Slides were examined using differential interference contrast (DIC) or epifluorescence optics for GFP, staining with fluorescent brightener 28 (calcofluor; CAL) and 4'-diamidino-2-phenylindole staining (DAPI) and viewed on a Reichart Jung Polyvar II microscope. Images were captured using a SPOT CCD camera (Diagnostic Instruments) and processed in Adobe Photoshop™ 5.0.

Results

The *P. marneffei* RAC homolog

The *P. marneffei* RAC homolog was cloned by low-stringency hybridization using the *P. marneffei* *CDC42* homolog *cflA*. The gene was named *cflB* (*Cdc42-like gene B*) and spans an open reading frame of 813 bp, consisting of five exons and four introns. Intron-exon junctions were confirmed by sequencing two cDNA clones isolated from a yeast 37°C cDNA library. The *cflB* gene encodes a predicted protein of 199 amino acids with high similarity to members of the Rho family of GTPases and specifically to the RAC subfamily. The conserved sequence TKLD is present at positions 121-124. This sequence is present in all RAC-like proteins and is TQXD in *CDC42* homologs and NKXD in other related Rho GTPases (Chen et al., 1993). CflB is most closely related to the Rho3 GTPase from *Aspergillus fumigatus* (AAG12157), which also contains the Rac-specific sequence TKLD (84% identity; 87% similarity). The *cflB* gene also shows sequence similarity to the RAC homologs from

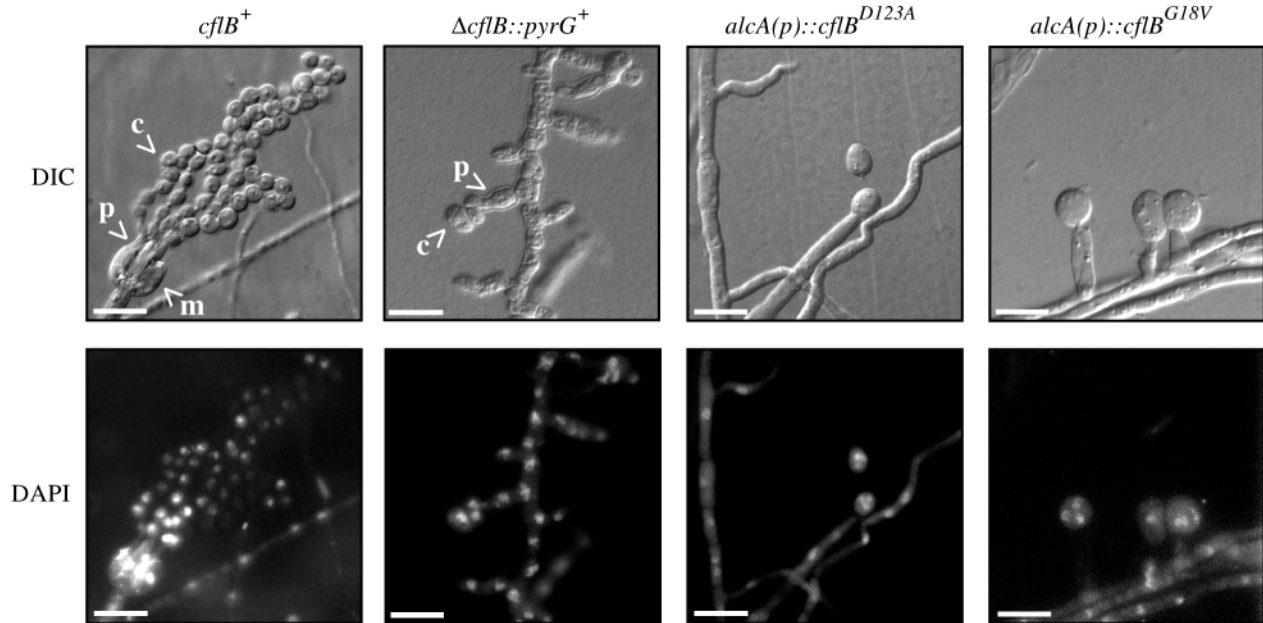


Fig. 4. *P. marneffei* *cfIB* controls polarity during asexual development at 25°C. Strains were grown for 4 days at 25°C (*cfIB*⁺ and Δ *cfIB*::*pyrG*⁺) or induced by 2 days of growth followed by induction for an additional day [*alcA*(*p*)::*cfIB*^{D123A} and *alcA*(*p*)::*cfIB*^{G18V}]. The arrowheads indicate conidiophore structures (c, conidia; m, metulae; p, phialides). The Δ *cfIB* strain produces aberrant conidiophores with swollen cells, which prevents the identification of the various conidiophore cell types. The *alcA*(*p*)::*cfIB*^{D123A} dominant-negative and *alcA*(*p*)::*cfIB*^{G18V} dominant-activated transformants also produce aberrant conidiophores. A singular swollen terminal conidium was observed in which there were multiple nuclei. Scale bar, 20 μ m. Images were captured using DIC or DAPI (to observe nuclei).

Magnoportha grisea (AF267176) and *Suillus bovinus* (AF235004).

The predicted protein sequence of CflB contains the domains previously shown to be necessary for GTPase function. These include the proposed GTP-binding and hydrolysis domains (GDGAVGKT and DTAGQE), a GDP to GTP exchange domain (TKLD), a domain for effector interaction (TVFDNY), and a C terminal CAAX motif (where A indicates an aliphatic amino acid and X any amino acid), which is predicted to allow association with the plasma membrane after prenylation (Ohya et al., 1993; Ziman et al., 1991; Chen et al., 1993).

Cellular localization of CflB

A *gpdA*(*p*)::*gfp*::*cfIB* fusion construct (pKB5441) was generated and co-transformed with the pAB4342 (*pyrG*) selectable plasmid into strain SPM4. Southern-blot analysis of DNA from four GFP fluorescent positive transformants showed that they had copy numbers of between 6 and 11 (data not shown). After 2 and 4 days of growth at 25°C, the fusion protein was clearly localized around the entire cell periphery, at internal membranes and at septa in both vegetative hyphae (Fig. 1A,B) and the asexual development structures (data not shown) of all cells. In yeast cells, after 4 days at 37°C, the GFP::CflB fusion protein was also localized around the cell periphery, at internal membranes and at septa in all cells (data not shown). To investigate the timing of CflB localization to septation sites, the GFP::CflB fusion protein and actin were localized in these strains using immunocytochemistry with anti-actin and anti-GFP antibodies. During hyphal growth,

after 4 days at 25°C, actin was localized as cortical spots along the length of hyphae and concentrated at the hyphal apex (Fig. 1C). Actin also formed structures at nascent septation sites (Fig. 1D). These structures constricted as the cell wall was laid down and actin was not detectable in mature septa. The GFP::CflB fusion protein co-localized with actin at nascent septation sites (Fig. 1D). In this case, the GFP::CflB fusion protein also co-localized with actin at the hyphal apex, presumably because of the increased sensitivity of immunostaining (Fig. 1C).

Expression of *cfIB*

Northern-blot analysis revealed that *cfIB* produced three differently expressed transcripts of approximately 1.0 kb, 1.1 kb and 1.3 kb in size (Fig. 2A). Both the 1.1 kb and the 1.3 kb *cfIB* transcripts were expressed under all tested conditions, whereas the 1.0 kb transcript was only expressed in vegetative hyphae and yeast cells. The 1.1kb transcript was the most abundant transcript under all conditions and the levels were higher at 37°C than 25°C.

RNA was also isolated from yeast cells grown for 8 days at 37°C then transferred to 25°C and incubated for 6 hours, 18 hours or 24 hours. During this time course, *P. marneffei* undergoes the yeast to hyphal dimorphic transition. Northern-blot analysis showed that the levels of the 1.1 kb and 1.0 kb *cfIB* transcripts initially increased and then decreased (Fig. 2B), indicating that *cfIB* undergoes a modest increase in expression during the morphological changes accompanying the 37°C to 25°C dimorphic switch.

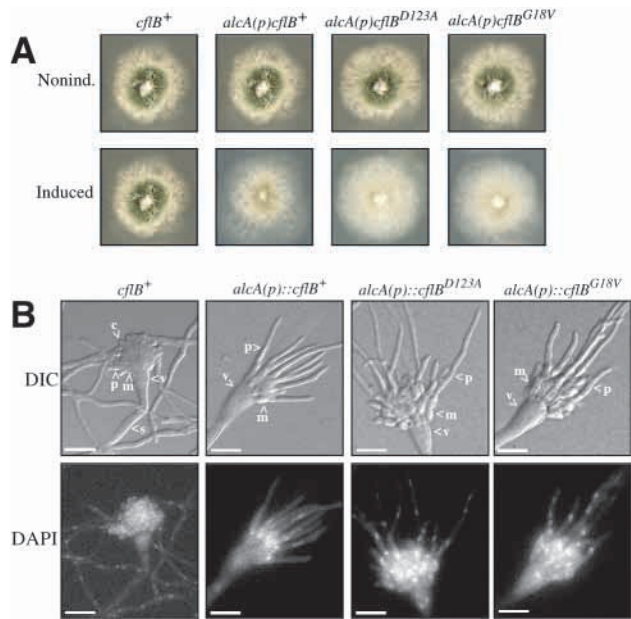


Fig. 5. The *cflB* gene affects asexual development in *A. nidulans*. (A) Colonial morphology of *A. nidulans cflB* strains. Strains were grown for 2 days at 25°C on noninducing (nonind.) or inducing (induced) medium. The *alcA(p)::cflB*, *alcA(p)::cflB*^{D123A} dominant-negative and *alcA(p)::cflB*^{G18V} dominant-activated transformants displayed a decrease in conidiation under inducing conditions that was more severe in the transformants with dominant alleles. (B) Strains were induced during conidiation by growth for 1 day at 25°C and induction for an additional day. The arrowheads indicate conidiophore structures (c, conidia; m, metulae; p, phialides; v, vesicle). The *alcA(p)::cflB*⁺, *alcA(p)::cflB*^{D123A} and *alcA(p)::cflB*^{G18V} transformants showed conidiophores with inappropriate polarized growth where metulae and phialides could be greatly extended. Scale bars, 20 μm. Images were captured using DIC or DAPI (to observe nuclei).

Disruption of *cflB* function

A deletion strain was generated by transformation of *P. marneffei* with the targeted deletion construct pKB4947, in which sequences encoding amino acids 28-52 of CflB were replaced with the *A. nidulans pyrG* selectable marker. *PyrG*⁺ transformants were screened by Southern-blot analysis and two strains were identified that showed genomic alterations consistent with replacement of the *cflB* locus with the *pyrG* deletion construct.

At 25°C, wild-type *P. marneffei* colonies consist of vegetative hyphae, aerial hyphae and conidiophores. The colonies are green because of the presence of asexual spores (conidia) produced by conidiophores. The $\Delta cflB$ strain produced abundant aerial hyphae, resulting in a fluffy phenotype and, although these colonies clearly produced conidia (the colony surface appeared green), they lacked visible conidiophore structures (Fig. 3A). To confirm that the phenotypes of the $\Delta cflB$ strain were due to the disruption of *cflB* and not to an unlinked mutation, a $\Delta cflB::pyrG^-$ strain was isolated by counterselection against *pyrG*⁺ on 5-fluoroorotic acid (Materials and Methods). This strain was transformed with pKB5236, containing the *cflB* gene and *pyrG*⁺ (Materials and Methods). All transformants isolated showed full complementation of the aerial hyphae and conidiophore defect.

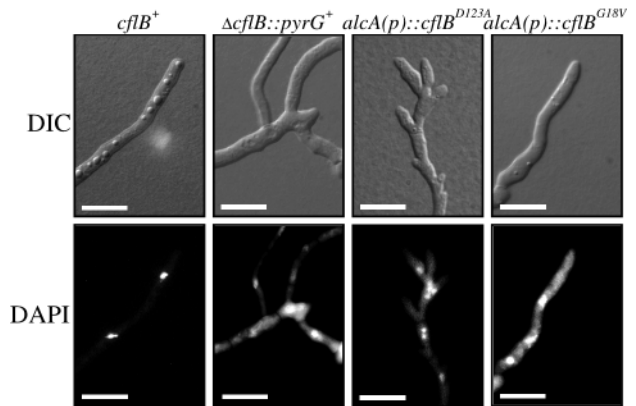


Fig. 6. Loss of *cflB* leads to an increase in apical branching in vegetative hyphal cells. Strains were grown for 2 days at 25°C (*cflB*⁺ and $\Delta cflB::pyrG^+$) or for 1 day and induced for an additional day [*alcA(p)::cflB*^{D123A} and *alcA(p)::cflB*^{G18V}]. Apical hyphal cells in the wild type are not branched. The $\Delta cflB$ and *alcA(p)::cflB*^{D123A} dominant-negative strains showed hyperbranched apical hyphal cells. The *alcA(p)::cflB*^{G18V} dominant-activated transformants possessed unbranched apical cells that displayed slightly irregular morphology. Scale bars, 20 μm. Images were captured using DIC or DAPI (to observe nuclei).

In addition to the null allele $\Delta cflB$, dominant-negative *cflB*^{D123A} and dominant-activated *cflB*^{G18V} mutant alleles were generated. The D123A mutation is located in a conserved position that, when mutated in other small GTPases, results in a dominant-negative phenotype, whereas the G18V mutation in small GTPases (including *RAC* homologs) gives rise to a dominant-activated phenotype because the mutant protein is unable to hydrolyse GTP and constitutively interacts with downstream effectors (Davis et al., 1998; Fanto et al., 2000; Kawaski et al., 1999; Kost et al., 1999). Both mutant alleles, as well as a wild-type allele were placed behind the ethanol-inducible *alcA* promoter from *A. nidulans* (May, 1987). The *alcA(p)::cflB* (pKB5021), *alcA(p)::cflB*^{D123A} (pKB5266) and *alcA(p)::cflB*^{G18V} (pKB5263) constructs were transformed into strain SPM4 and four representative *pyrG*⁺ transformants for each *cflB* construct were analysed further. The copy number of these strains ranged from three to eight for *alcA(p)::cflB*, from one to ten for *alcA(p)::cflB*^{D123A} and from two to three for *alcA(p)::cflB*^{G18V}. No phenotypic effects caused by copy number were evident in these transformants. Overexpression of *cflB* (*alcA(p)::cflB*) had no detectable phenotype (Fig. 3B). By contrast, the dominant-negative *alcA(p)::cflB*^{D123A} strains showed a slightly fluffy phenotype under inducing conditions, with conidiophores that were reduced in height (Fig. 3B). This phenotype was similar to the $\Delta cflB$ strain, albeit less severe. The dominant-activated *alcA(p)::cflB*^{G18V} strains showed non-uniform conidiation across the colony on inducing medium (Fig. 3B). Under non-inducing conditions, all strains had a wild-type phenotype.

cflB is required for asexual development in *P. marneffei*

The differentiation of hyphal cells during asexual development requires regulated changes in polarized growth. *P. marneffei* initiates asexual development with the production of a specialized cell type (stalk) from a vegetative hyphal cell.

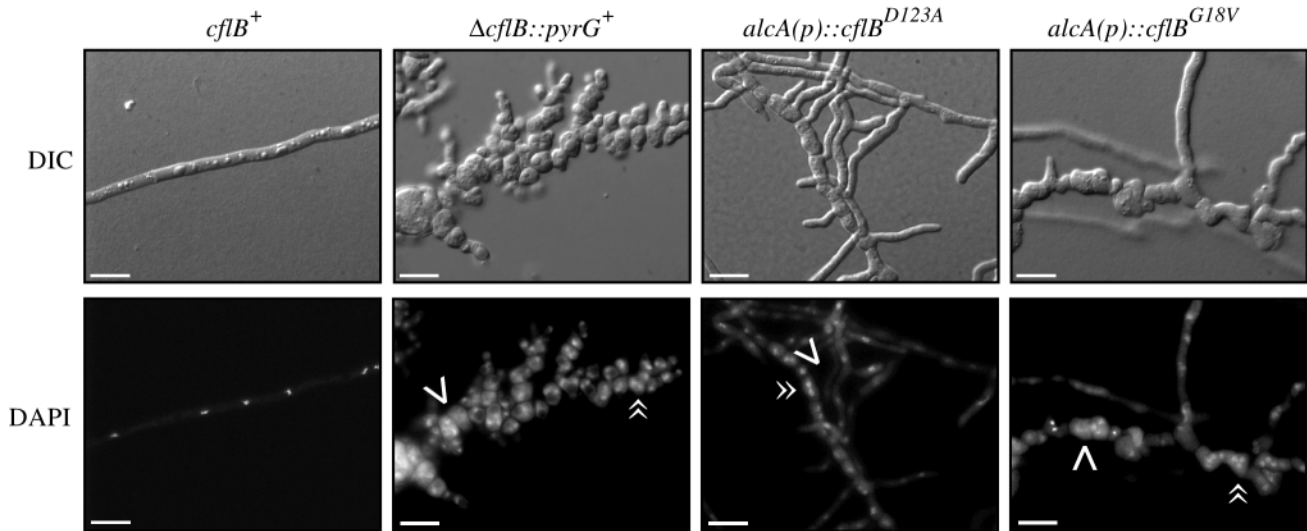


Fig. 7. *cfB* is necessary for polarized growth of vegetative hyphal cells. Strains were grown for 4 days at 25°C (*cfB*⁺ and $\Delta cfB::pyrG^+$) or for 2 days and induced for an additional day [*alcA(p)::cfB*^{D123A} and *alcA(p)::cfB*^{G18V}]. The ΔcfB strain displays extremely swollen hyphal cells that can be anucleate, uninucleate or multinucleate. The *alcA(p)::cfB*^{D123A} dominant-negative and *alcA(p)::cfB*^{G18V} dominant-activated transformants also possess swollen hyphal cells but depolarized to a lesser extent than ΔcfB . Hyphal cells can also be anucleate, uninucleate or multinucleate. Single arrowheads indicate anucleate hyphal cells and double arrowheads indicate multinucleate hyphal cells. Scale bars, 20 μ m. Images were captured using DIC or DAPI (to observe nuclei).

Sequential budding at the apical end of the stalk produces sterigmata (metulae and phialides). The sporogenic phialide cells bud at the apical tip to produce conidia (Borneman et al., 2000). The conidiation defects evident in the ΔcfB , *alcA(p)::cfB*^{D123A} and *alcA(p)::cfB*^{G18V} strains at the colonial level (Fig. 3) were analysed further microscopically. At 25°C, after 4 days, although conidia were present in the ΔcfB strain, conidiophores were not easily distinguishable because the metulae and phialides were swollen and misshapen, and were occasionally multinucleate (Fig. 4).

Under inducing conditions, the dominant-negative *alcA(p)::cfB*^{D123A} strains displayed conidiophores with a single, terminal, swollen, multinucleate conidium (Fig. 4). Occasionally, branched conidiophores were also observed (not shown). The dominant-activated *alcA(p)::cfB*^{G18V} strains also displayed conidiophores with a single, swollen, multinucleate conidium (Fig. 4). However, unlike the *alcA(p)::cfB*^{D123A} strains, branched conidiophores were not observed.

Correct *cfB* function is required for asexual development in *A. nidulans*

To determine whether the function of CflB is conserved in other fungi, the *alcA(p)::cfB* (pKB5021), *alcA(p)::cfB*^{D123A} (pKB5266) and *alcA(p)::cfB*^{G18V} (pKB5263) constructs were transformed into an *A. nidulans pyrG*⁻ strain. Transformants carrying any of these *cfB* alleles exhibited a severe decrease in conidiation under inducing conditions and no detectable change in phenotype under non-inducing conditions (Fig. 5). In all of the *A. nidulans cfB* transformants, conidiophores displayed inappropriate polarized growth such that metulae and phialides could be greatly extended in length and were often multinucleate (Fig. 5). Although these extended cells were multinucleate, they were not septate and failed to conidiate.

These strains produced conidia exclusively from conidiophores with wild-type morphology. In addition to the conidiation phenotype, the *A. nidulans alcA(p)::cfB*^{D123A} transformants also exhibited polarization defects in the vegetative hyphae. Hyphal cells were occasionally swollen, consequently appearing reduced in length, and apical cells could be multibranching (data not shown).

Deletion of *cfB* affects germination and results in misshapen conidia

Wild-type *P. marneffei* conidia are activated and begin isotropic growth after 6 hours at 25°C under appropriate growth conditions. After 8 hours, the conidia become highly polarized and, after 12 hours, a germ tube emerges. Growth at this stage is directed exclusively to the germ-tube apex. Secondary germ tubes emerge from the conidium after ~15 hours incubation at 25°C. Conidia of the ΔcfB strain were incubated for 12 hours or 15 hours at 25°C, and germ-tube emergence was measured by counting the number of germlings with primary, secondary or tertiary germ tubes in a population of 100 over three independent experiments. After 12 hours, wild-type *P. marneffei* had 78.3% (± 0.88) conidia with primary germ tubes, 20% (± 0.58) conidia with secondary germ tubes and 1.67% (± 0.67) conidia with tertiary germ tubes. By contrast, ΔcfB conidia exhibited an increased rate of secondary germ-tube emergence with 70.3% (± 2.02) primary germ tubes and 26.3% (± 0.88) secondary germ tubes. The proportion of ΔcfB conidia with a tertiary germ tube was 3.33% (± 1.86), which does not differ from the wildtype.

After 15 hours at 25°C, 99.7% (± 0.33) of wild-type conidia had germinated (polarized, with one or more germ tubes) and only 0.33% (± 0.33) remain ungerminated. By contrast, the ΔcfB strain had 20.3% (± 1.33) conidia that remained

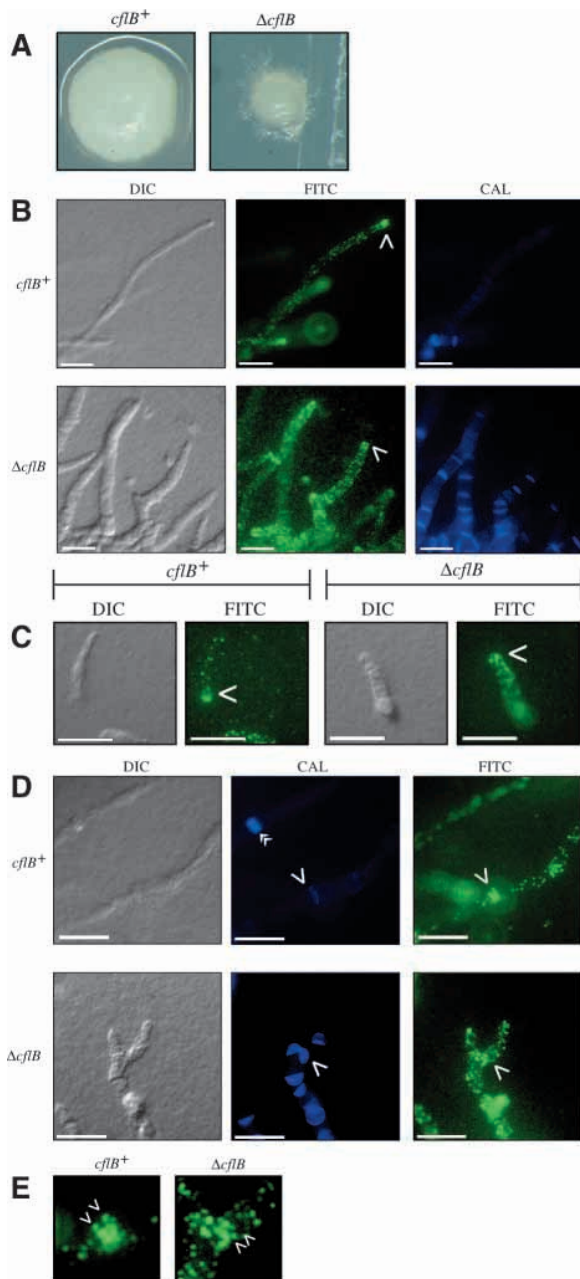


Fig. 8. The *cflB* gene is not required for correct actin localization in arthroconidiating hyphae and in yeast cells. Wild-type and $\Delta cflB$ strains were grown for 4 days at 37°C. Actin localization was examined using immunocytochemistry. (A) Colonial morphology at 37°C. Colonies of the $\Delta cflB$ strain are reduced in size and possess irregular edges. (B) Arthroconidiating hyphae are shown at 37°C prior to cell separation. The $\Delta cflB$ strain possesses swollen arthroconidiating hyphae that are highly septate. The white arrows indicate concentrated actin in both wild-type and $\Delta cflB$ strains. (C) Yeast cells at 37°C. The single white arrow indicates actin concentrated in a yeast cell of both the wildtype and the $\Delta cflB$ strain. (D) Nascent septation sites in vegetative hyphae at 37°C. Two regions of concentrated actin are indicated by single white arrows in the FITC panel. The corresponding cell wall is indicated by a single arrow in the CAL panel. Double arrows indicate completed double septation sites. (E) Magnification of the actin staining regions marked in D, where the arrows indicate the two regions of concentrated actin. Scale bars, 20 μ m.

ungerminated after 15 hours. In addition, unlike the uniform ellipsoidal shape of wild-type conidia (ungerminated or isotropically polarized), 37.5% (± 2.22) of germinated $\Delta cflB$ conidia were misshapen. The low germination percentage and abnormal morphology could be attributed either to defects during conidiophore development or germination.

CflB controls polarized growth of vegetative cells at 25°C

At 25°C, the SPM4 control strain produced hyphae by the highly polarized growth of apical cell tips, followed by septation and by the emergence of new growth tips in subapical cells. Apical cells were never branched and extended exclusively by polarized growth at the apical tip and septation occurred at regular intervals. After 2 days growth at 25°C, the $\Delta cflB$ strain displayed apical branching and often showed multiple branches extending from a single apical cell (Fig. 6). In the wildtype, subapical hyphal cells were $\sim 40 \pm 5$ μ m in length and produce a single branch. By contrast, the $\Delta cflB$ mutant extended multiple branches from subapical cells and these branches were also often branched. Under inducing conditions, the dominant-negative *alcA(p)::cflB^{D123A}* transformants also showed branched apical hyphal cells and hyperbranching of subapical hyphal cells (Fig. 6). By contrast, the *alcA(p)::cflB* and *alcA(p)::cflB^{G18V}* strains showed wild-type branching patterns under inducing conditions. In the wildtype, nuclei were evenly distributed along a hypha, with older subapical hyphal cells containing a single nucleus and apical cells containing multiple nuclei. The nuclear distribution of all of the *cflB* mutant strains did not differ from the wildtype after 2 days.

After 4 days of growth, the older cells (subapical) showed a reduction in hyphal cell length to $\sim 20 \pm 2$ μ m. The $\Delta cflB$ strain showed aberrant swollen subapical cells that appeared to be severely reduced in length (5 ± 2 μ m) (Fig. 7). Subapical cells did not exhibit polarized growth, except during the initiation of new branches. Thus, it appears that the deletion of *cflB* results in either inappropriate growth or disruption of cell integrity, which leads to cell swelling. Staining of cell walls using calcofluor showed septal positioning defects. Septa were in close proximity, orientated along random planes rather than perpendicular to the long axis of the cell and greatly thickened compared to the wildtype. The nuclear index of these cells varied from none to many (>10 nuclei). Many apical and subapical hyphal cells were hyperbranched and swelling in hyphal cells varied between cells (Fig. 7). Under inducing conditions, the *alcA(p)::cflB^{D123A}* dominant-negative transformants also displayed swollen hyphal cells (10 ± 5 μ m), although to a lesser extent than the $\Delta cflB$ strain, with fewer anucleate or multinucleate subapical cells and hyperbranched subapical and apical cells (Fig. 7). The *alcA(p)::cflB^{G18V}* transformants showed misshapen swollen hyphae of varied length (15 ± 10 μ m) and nuclear index (Fig. 7). By contrast, the *alcA(p)::cflB* strain showed a wild-type phenotype.

Deletion of *cflB* does not affect yeast cell production

P. marneffeii is dimorphic, growing in a filamentous multinucleate hyphal form at 25°C or in a uninucleate yeast form at 37°C. The initial stage of conidial germination and

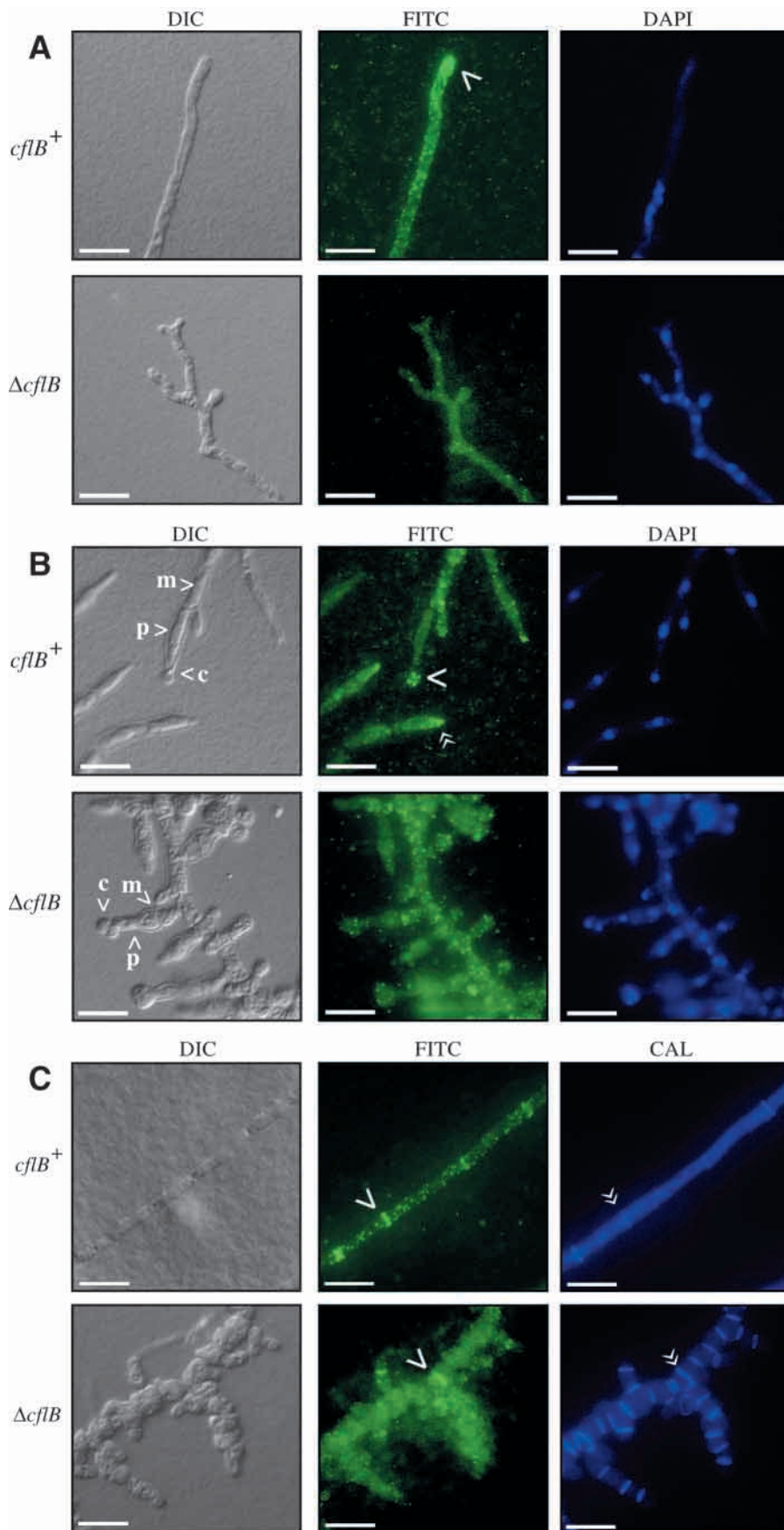


Fig. 9. The *cflB* gene is necessary for correct actin localization in vegetative hyphal cells. Strains were grown for 4 days at 25°C. Actin localization was examined using immunocytochemistry. Actin is localized as cortical spots and is also concentrated at sites of polarized growth. (A) Vegetative hyphal growth at 25°C. The white arrow indicates concentrated actin at the hyphal apex, which is absent in the $\Delta cflB$ strain. (B) Asexual development at 25°C. The single white arrow indicates actin concentrated in the newly formed conidium, the double white arrow indicates actin concentrated at the distal tip of a phialide. Conidiophore cell types are indicated (c, conidia; m, metulae; p, phialides). The $\Delta cflB$ strain lacks actin concentrated in conidiophores. (C) Nascent septation sites in vegetative hyphae at 25°C. Concentrated actin is indicated by single white arrows (FITC panel) and double arrows indicate corresponding cell walls (CAL panel). Scale bars, 20 μ m.

polarized growth in *P. marneffei* does not appear to differ significantly at either 25°C or 37°C. Conidia expand isotropically and then become highly polarized to produce a hypha that grows by apical extension and divides by septation. However, after 4 days at 25°C, the hyphae begin to develop asexual structures, whereas, after 4 days at 37°C, *P. marneffei* undergoes arthroconidiation, which results in the production of rod-shaped yeast cells (arthroconidia). Double septa are laid down in hyphae and fragmentation occurs along the septal plane to generate single cells (Chan and Chow, 1990). The liberated yeast cells are uninucleate, $\sim 20 \pm 2$ μ m in length and divide by fission (Chan and Chow, 1990).

After 4 days at 37°C, wild-type *P. marneffei* yeast colonies possess uniform edges (Fig. 8A). When the $\Delta cflB$ strain was grown for 4 days at 37°C, colonies were greatly reduced in size and displayed irregular edges (Fig. 8A). When analysed microscopically, the arthroconidiating hyphae of the $\Delta cflB$ strain appeared larger in diameter than the wildtype (Fig. 8B, DIC panel). In addition, the arthroconidiating hyphae of the $\Delta cflB$ strain possessed more nuclei per cell and were highly septate (Fig. 8B, CAL panel). Compared with the wildtype, arthroconidiation appeared more complete in the $\Delta cflB$ strain, with few true hyphae evident. Despite the aberrations in cell morphology of the

ΔcflB arthroconidiating hyphae, normal yeast cells were produced (Fig. 8C).

CflB is required for actin localization during vegetative growth and asexual development

The cell-polarity defects evident in *ΔcflB* mutant strain might be the result of disruption in the actin cytoskeleton because Rac proteins have been implicated in actin-mediated morphogenesis in several organisms. We examined the effect of loss of *cflB* on actin organization in the various cell types of *P. marneffei* using a mouse anti-actin antibody (see Materials and Methods). During hyphal growth of wild-type *P. marneffei* at 25°C, actin was localized in cortical spots along the length of hyphae and concentrated at actively growing branches and hyphal tips (Fig. 9A). Actin was present at the nascent septation site before the cell wall was visible (detected by the calcofluor cell-wall stain). The amount of actin observed decreased as the septum wall was laid down and mature septa did not appear to contain actin (Fig. 9C). During asexual development, actin was concentrated at sites of active cellular morphogenesis and division at the distal tips of stalks, metulae and phialides, and the nascent conidium bud sites (Fig. 9B). Cortical actin and actin at sites of septation were evident in the *ΔcflB* strain, although concentrated actin patches at the hyphal tips were absent (Fig. 9A,C). Thus, CflB is required for actin localization at the hyphal tip but not for localization of cortical spots and actin at nascent septation sites. During asexual development, the *ΔcflB* strain produced conidiophores that were swollen and aberrant in all sterigmata cells. Actin in conidiophore cells of the *ΔcflB* strain was not localized in developing metulae, phialides or conidia, suggesting correct actin localization by *cflB* is required for morphogenesis of these developmental cell types (Fig. 9B).

During growth of wild-type *P. marneffei* at 37°C, actin localized in cortical spots along the arthroconidiating hyphae and was concentrated at the hyphal tip (Fig. 8B). Similar to what was observed at 25°C, actin formed structures at nascent septation sites and these were reduced as the cell wall was laid down and were absent in mature septa. At some septation sites, a second actin structure was formed as the first reduced and the first septal wall was laid down. Subsequently, this second actin structure disappeared as the second septal wall was laid down (Fig. 8D). Yeast cells that had separated from the arthroconidiating hyphae showed concentrated actin at one end of the cell (Fig. 8C). Despite the *ΔcflB* strain possessing swollen arthroconidiating hyphae with increased septation, actin was still correctly localized in yeast cells (Fig. 8B-D).

Discussion

Correct cellular targeting is essential for the function of Rho GTPases (Ohya et al., 1993). One aspect of Rho GTPase function is to localize effectors and other proteins required for polarization to the imminent growth site (Johnson, 1999). We found that CflB was localized at the plasma membrane, at internal membranes and at septation sites. CflB was predicted to localize to the plasma membrane owing to the presence of a poly-lysine domain at positions 190-195 (KNKAKR) and a C-terminal CTIL CAAX box. The localization of CflB suggests that these motifs are active. Cdc42 proteins have been

localized in a number of organisms and this localization is similar to that observed for *P. marneffei* CflB. In *S. cerevisiae* and *S. pombe*, Cdc42p is localized to the plasma and internal membranes and geranylgeranylation of the Cys¹⁸⁸ residue of *S. cerevisiae* Cdc42p is necessary for membrane attachment and function (Richman et al., 2002; Merla and Johnson, 2000). The CAAX box is sufficient for localization to internal membranes and both the CAAX box and poly-lysine domain were sufficient for localization to the plasma and internal membranes (Richman et al., 2002). The function of Cdc42p at internal membranes is not clear, although there is some evidence that Cdc42p in *S. cerevisiae* plays a role in endocytosis and vacuolar fusion (Eitzen et al., 2001; Muller et al., 2001). The localization of CflB to internal membranes might therefore indicate that CflB, and therefore RAC homologs in general, might be involved in a similar process.

It is currently unknown whether Rac proteins are involved in cellular division. Cdc42 in *S. cerevisiae* and *S. pombe* has been shown to be crucial for cytokinesis (Johnson, 1999). If Rac proteins were also involved in cytokinesis, it would be expected that the protein be localized at division sites. We observed that, in *P. marneffei*, CflB was localized at septation sites suggesting that Rac homologs like Cdc42 have a functional role during cellular division. This was also supported by the phenotype of the *ΔcflB* mutant, which displayed severe septal positioning defects. It is unclear whether the septal positioning defects are due to inappropriate cleavage of previously established compartments or inappropriate spacing when septa are first deposited. In *S. cerevisiae*, Cdc42p is localized to the mother-bud junction and, in *S. pombe*, Cdc42p is clustered at the site of cell division (Merla and Johnson, 2000; Richman et al., 1999). In the ectomycorrhizal hyphae of *S. bovinus*, Cdc42 is evident as two opposing spots at the plasma membrane preceding actin formation at the nascent septation site and this suggests that Cdc42 in *S. bovinus* acts early during cellular division before the formation of the actin ring (Gorfer, 2001). By contrast, we found that CflB in *P. marneffei* is colocalized as rings with actin at nascent septation sites, suggesting that Rac proteins play a role later in division.

Because Rac proteins are involved in polarized growth, CflB was expected to be concentrated at sites of polarized growth such as the hyphal tip. This was not evident in live cells but was detected by immunocytochemistry, presumably because of the higher sensitivity of this method. In *S. cerevisiae*, Cdc42p is clustered at sites of polarized growth, such as incipient bud sites and the tips and sides of enlarging buds, and this site changes depending on the stage of the cell cycle (Richman et al., 2002; Ziman, 1993). Cdc42p in *S. pombe* was not found to be concentrated at the cell tips (Merla and Johnson, 2000). The CflB localization data suggest that CflB plays a role during polarized growth. Loss of correct CflB function resulted in a loss of polarized growth of vegetative hyphae, with hyphae becoming swollen and misshapen and a loss of concentrated actin at the hyphal tip. Therefore, CflB acts to maintain polarized growth by directly or indirectly localizing actin at the growth site. In addition, both the deletion and dominant-negative strains displayed hyperbranching of apical and subapical hyphal cells. These data suggest that hyperbranching occurs because of the lack of correctly focused actin at active apical cells. In the absence of concentrated actin, growth is not

directed and so cells grow in multiple directions. Alternatively, CflB might negatively control proteins required to initiate a new site of polarized growth, and loss of CflB function results in constitutive activity of these factors. This suggests that another protein takes over after the CflB polarization signal is received, which is consistent with the phenotype of the dominant-activated transformants, which have branching patterns similar to the wildtype.

Asexual conidiation is a developmental process that requires, with the exception of the stalk, the sequential budding of apical cells (Borneman et al., 2000). Budding requires the regulated switching on and off of polarized growth in synchrony with the nuclear division cycle, and the dynamic reorganization of the actin cytoskeleton. It is clear that CflB, in addition to regulating polarized growth of vegetative hyphae, also plays a role in regulating polarized growth during asexual development. All mutant *cflB* strains showed conidiation defects and in particular, conidiophores of the $\Delta cflB$ strain were swollen, aberrantly shaped and lacked localized actin. These results suggest that CflB regulates polarized growth during asexual development by regulating actin organization. The dominant-negative transformants, in which the mutant protein is locked in the GDP-bound inactive form, have conidiophores with reduced length and complexity that have failed to undergo correct polarized growth, supporting the suggestion that CflB plays a positive role during polarized growth. Interestingly, reduced conidiophores are also observed in the *P. marneffeii* dominant-activated transformants. If CflB acts to turn on polarized growth, it might be expected that the dominant-activated transformants would have continuous polarized growth, owing to the inability to convert the mutant protein into the GDP-bound inactive form. Therefore, not only must polarized growth be turned on by active GTP-bound CflB but the CflB protein must be able to cycle appropriately between a GDP-bound and a GTP-bound form.

Rac proteins have been shown to positively regulate polarized growth in other organisms. When the *Y. lipolytica* RAC homolog is deleted, an impairment of polarized growth in hyphal cells is seen (Hurtado et al., 2000). It has also been observed that correct cycling between the GDP- and GTP-bound forms is essential for positively regulating polarized growth. The expression of the dominant-negative RAC alleles in the nervous system of *D. melanogaster* resulted in occasional loss of axons between the dorsal and lateral clusters of the peripheral nervous system. Expression of the dominant-activated allele resulted in a more severe phenotype, with axons missing between the dorsal and lateral clusters in most segments, in addition to loss of axons connecting the lateral and ventral clusters (Luo et al., 1996). Therefore, the general function of Rac proteins is to positively regulate polarized growth by cycling between an inactive and active form, and this is conserved between distantly related organisms.

We were interested in determining whether Rac proteins function in the same manner in the analogous process in a closely related organism. The process of asexual development in *A. nidulans* is similar to *P. marneffeii*. In both fungal species, a stalk is produced from the vegetative hyphae but, in *A. nidulans*, this stalk swells to produce the vesicle. Both organisms then undergo sequential budding of cells from the stalk or vesicle to produce the sterigmata and conidia (Timberlake, 1987; Borneman et al., 2000). In *A. nidulans*,

overexpression of the wild-type and mutant *cflB* alleles resulted in conidiophores that showed hyperpolarized growth. This occurred in both metulae and phialides, and resulted in multinucleate cells that remained aseptate. This suggests that, in contrast to *P. marneffeii*, *A. nidulans* Rac might function to turn off polarized growth during asexual development. The difference in the regulation of polarized growth during asexual development in *A. nidulans* and *P. marneffeii* also extends to other Rho GTPases. *A. nidulans* transformants expressing mutant *cflB* alleles show hyperpolarization of conidiophores, whereas overexpression of the *P. marneffeii* CDC42 homolog *cflA* in *A. nidulans* completely blocks conidiation (Boyce, 2001). In *P. marneffeii*, expression of dominant-negative or -activated *cflB* alleles reduces polarized growth during conidiation but, when the dominant-negative or -activated *cflA* alleles are expressed, conidiation is not affected. This highlights the fact that, although small GTPases are highly conserved in structure and ability to regulate actin, they can regulate processes differently even in closely related organisms. It is interesting that the yeasts *S. cerevisiae* and *S. pombe*, and filamentous fungus *A. gossypii* do not have Rac orthologs (<http://genome-ftp.stanford.edu/pub/yeast/>; <http://nucleus.cshl.edu/pombeweb/>; P. Philippsen, personal communication). The evolution of complicated developmental programs in higher eukaryotes might have required the evolution of two proteins that perform similar yet specialized functions. In support of this, the dimorphic yeasts *Y. lipolytica* and *Candida albicans*, and the complex filamentous fungi *A. fumigatus* and *P. marneffeii* do possess Rac orthologs and these organisms show a larger repertoire of morphogenetic events (Hurtado et al., 2000; Alexopoulos et al., 1996). In the case of *C. albicans*, the Rac has a non-conserved TKVD sequence (<http://www-sequence.stanford.edu/group/candida>).

How small GTPases coordinately regulate different aspects of development is of continuing interest. In *P. marneffeii*, the Cdc42 and Rac proteins possess coordinate roles during development. Both CflA and CflB are required for vegetative growth at 25°C, although the roles appear to be distinct because the phenotypes are not identical (Boyce et al., 2001). CflA and CflB also possess distinct roles during development. CflA is required for yeast cell morphology at 37°C but is not required during asexual development at 25°C (Boyce et al., 2001). By contrast, CflB is not required for yeast cell morphogenesis but is required during asexual development. In other organisms, Rho GTPases also possess distinct roles in morphogenesis. For example, the expression of the dominant activated allele of *DmRAC1* during nervous-system development resulted in stalling of axons, but dendrites were unaffected. When the dominant-activated *CDC42* allele was expressed, axons were missing and incorrectly positioned, and, in addition, dendrites were abnormal or absent (Luo et al., 1994). Understanding the molecular basis for this coordination will greatly enhance our understanding of how actin organization and morphogenesis are regulated throughout development.

This work was supported by a grant from the Australian Research Council. K.J.B. was supported by an Australian Postgraduate Award (APA) scholarship.

References

- Alexopoulos, C. J., Mims, C. W. and Blackwell, M. (1996). *Introductory Mycology*. New York: John Wiley and Sons.
- Ausubel, F. M., Brent, R., Kingston, R. E., Moore, D. D., Seidman, J. A., Smith, J. A. and Struhl, K. (1994). *Current protocols in molecular biology*. New York: John Wiley and Sons, Inc.
- Borneman, A. R., Hynes, M. J. and Andrianopoulos, A. (2000). The *abaA* homolog of *Penicillium marneffei* participates in two developmental pathways: conidiation and dimorphic growth. *Mol. Microbiol.* **38**, 1034-1047.
- Borneman, A. R., Hynes, M. J. and Andrianopoulos, A. (2001). A *STE12* homolog from the asexual, dimorphic fungus *Penicillium marneffei* complements the defect in sexual development of an *Aspergillus nidulans* *steA* mutant. *Genetics* **157**, 1003-1014.
- Boyce, K. J., Hynes, M. J. and Andrianopoulos, A. (2001). The *CDC42* homolog of the dimorphic fungus *Penicillium marneffei* is required for correct cell polarization during growth but not development. *J. Bacteriol.* **183**, 3447-3457.
- Chan, Y. F. and Chow, T. C. (1990). Ultrastructural observations on *Penicillium marneffei* in a natural human infection. *Ultrastruct. Pathol.* **14**, 439-452.
- Chant, J. and Stowers, L. (1995). GTPase cascades choreographing cellular behaviour: movement, morphogenesis, and more. *Cell* **81**, 1-4.
- Chen, W. N., Lim, H. H. and Lim, L. (1993). The *Cdc42* homolog from *Caenorhabditis elegans* – complementation of yeast mutation. *J. Biol. Chem.* **268**, 13280-13285.
- Davis, C. R., Richman, T. J., Deliduka, S. B., Blaisdell, J. O., Collins, C. C. and Johnson, D. I. (1998). Analysis of the mechanisms of action of the *Saccharomyces cerevisiae* dominant lethal *Cdc42(G12V)* and dominant negative *Cdc42(D118A)* mutations. *J. Biol. Chem.* **273**, 849-858.
- Eaton, S., Auvinen, P., Luo, L. Q., Jan, Y. N. and Simons, K. (1995). *Cdc42* and *Rac1* control different actin-dependent processes in the *Drosophila* wing disc epithelium. *J. Cell Biol.* **131**, 151-164.
- Eitzen, G., Thorngren, N. and Wickner, W. (2001). *Rho1p* and *Cdc42p* act after *Ypt7p* to regulate vacuole docking. *EMBO J.* **20**, 5650-5656.
- Fanto, M., Weber, U., Strutt, D. I. and Mlodzik, M. (2000). Nuclear signalling by *Rac* and *Rho* GTPases is required in the establishment of epithelial planar polarity in the *Drosophila* eye. *Curr. Biol.* **10**, 979-988.
- Fischer, R. and Timberlake, W. E. (1995). *Aspergillus nidulans* *apsA* encodes a coiled-coil protein required for nuclear positioning and completion of asexual development. *J. Cell Biol.* **128**, 485-498.
- Gorfer, M., Tarkka, M. T., Hanif, M., Pardo, A. G., Laitinen, E. and Raudaskoski, M. (2001). Characterization of small GTPases *Cdc42* and *Rac* and the relationship between *Cdc42* and actin cytoskeleton in vegetative and ectomycorrhizal hyphae of *Suillus bovinus*. *Mol. Plant-Microbe Interact.* **14**, 135-144.
- Hurtado, C. A. R., Beckerich, J., Gaillardin, C. and Rachubinski, R. A. (2000). A *Rac* homolog is required for induction of hyphal growth in the dimorphic yeast *Yarrowia lipolytica*. *J. Bacteriol.* **182**, 2376-2386.
- Johnson, D. I. (1999). *Cdc42*: an essential *Rho*-type GTPase controlling eukaryotic cell polarity. *Microbiol. Mol. Biol. Rev.* **63**, 54-105.
- Kost, B., Lemichez, E., Spielhofer, P., Hong, Y., Tolia, K., Carpenter, C. and Chua, N. (1999). *Rac* homologs and compartmentalized phosphatidylinositol 4,5-bisphosphate act in a common pathway to regulate polar pollen tube growth. *J. Cell Biol.* **145**, 317-330.
- Luo, L. Q., Liao, Y. J., Jan, L. Y. and Jan, Y. N. (1994). Distinct morphogenetic functions of similar small GTPases – *Drosophila* *dRAC1* is involved in axonal outgrowth and myoblast fusion. *Genes Dev.* **8**, 1787-1802.
- Luo, L. Q., Jan, L. and Jan, Y. N. (1996). Small GTPases in axon outgrowth. *Perspect. Dev. Neurobiol.* **4**, 199-204.
- May, G. S. (1987). Cloning, mapping and molecular analysis of the *pyrG* (orotidine-5'-phosphate decarboxylase) gene of *Aspergillus nidulans*. *Gene* **61**, 385-399.
- Merla, A. and Johnson, D. I. (2000). The *Cdc42p* GTPase is targeted to the site of cell division in the fission yeast *Schizosaccharomyces pombe*. *Eur. J. Cell Biol.* **79**, 469-477.
- Muller, O., Johnson, D. I. and Mayer, A. (2001). *Cdc42p* functions at the docking stage of yeast vacuole membrane fusion. *EMBO J.* **20**, 5657-5665.
- Nobes, C. D. and Hall, A. (1995). *Rho*, *Rac* and *Cdc42* GTPases regulate the assembly of multimolecular focal complexes associated with actin stress fibers, lamellipodia, and filopodia. *Cell* **81**, 53-62.
- Ohya, Y. H., Qadota, H., Anraku, Y., Pringle, J. R. and Bolstein, D. (1993). Suppression of yeast geranylgeranyl transferase I defect by alternative prenylation of two target GTPases, *Rho1p* and *Cdc42p*. *Mol. Biol. Cell* **4**, 1017-1025.
- Richman, T. J., Sawyer, M. M. and Johnson, D. I. (1999). The *Cdc42p* GTPase is involved in a G2/M morphogenetic checkpoint regulating the apical-isotropic switch and nuclear division in yeast. *J. Biol. Chem.* **274**, 16861-16870.
- Richman, T. J., Sawyer, M. M. and Johnson, D. I. (2002). *Saccharomyces cerevisiae* *Cdc42p* localizes to cellular membranes and clusters at sites of polarized growth. *Eukaryotic Cell* **1**, 458-468.
- Sambrook, J., Fritsch, E. F. and Maniatis, T. (1989). *Molecular Cloning, A Laboratory Manual*. Cold Spring Harbor, USA: Cold Spring Harbor Laboratory Press.
- Timberlake, W. E. (1987). Molecular genetic analysis of development in *Aspergillus nidulans*. *Dev. Biol.* **78**, 497-510.
- Ziman, M., Preuss, D., Mulholland, J., O'Brien, J. M., Botstein, D. and Johnson, D. I. (1993). Subcellular localization of *Cdc42p*, a *Saccharomyces cerevisiae* GTP-binding protein involved in the control of cell polarity. *Mol. Biol. Cell* **4**, 1307-1316.